Nonclassical fields in a linear directional coupler

W. K. Lai, V. Bužek,* and P. L. Knight
Optics Section, Blackett Laboratory, Imperial College, London, SW7 2BZ, England
(Received 10 December 1990)

In the present paper, we discuss the photon statistics of nonclassical fields in a linear directional coupler. We study the photon distributions at the output ports of the coupler for number-state inputs, as well as for arbitrary-state inputs. In particular, we show that when a number state enters one port of the coupler and the vacuum enters the other port, an SU(2) coherent state is generated at the output ports. If the same number state enters both ports of the coupler, the probability of finding an odd number of photons at either of the output ports vanishes for a particular choice of the coupler length. We show that if a number state enters port 1 and a strong coherent field enters port 2, the coupler can serve as a generator of displaced number states (in fact, in this case the coupler behaves essentially as a homodyne detector). We show that the coupler is equivalent to an imperfect photon detector with efficiency governed by the coupler parameters. We study the effect of dissipative losses within the coupler as well as the effect of scattering coupling in the coupler. The latter leads to equalization of the energy in each guide. We show that in the presence of scattering coupling, the coupler behaves neither like an imperfect photon detector nor a homodyne detector.

I. INTRODUCTION

Optical communications networks frequently require switching, modulation, and frequency selection of radiation fields. These tasks are commonly carried out by a linear directional coupler, a device consisting of two closely spaced optical waveguides. The overlap between the mode functions of the respective guides allows a controlled transfer of power from one guide to the other. Classical treatments of the coupler based on the coupled-mode theory have been given by many authors.[1] While these treatments are sufficient for many purposes, a quantum treatment becomes essential when the statistical properties of the radiation field are important. With this in mind, Janszky, Sibilia, and Bertolotti[2,3] used a quantum generalization of the classical field equations of motion to investigate the photon statistics of nonclassical light in a coupler. Using quasiprobability methods[4] they obtained relations between input and output quadrature variances for fields with complex statistics (i.e., fields having simultaneously coherent, chaotic, and squeezing characteristics), and showed in particular that a squeezed state may be switched from one guide to the other, without destroying the nonclassical properties of the state.[2] In a later paper[3] they then extended their analysis to photon number-state inputs. They showed that binomial photon distributions[5] can be obtained by launching a single photon-number state into one of the input ports of the coupler. The lossless linear directional coupler is of course related to a lossless beam splitter in the way it couples quantized field modes. Campos, Saleh, and Teich[6] have shown that states of light with a binomial counting distribution can be generated by the action of such a beam splitter on a nonclassical field, with the input in one port prepared in a number state while the second input is the vacuum state. The binomial partition of photons is of course well known (see, e.g., the review by Loudon,[7] and the earlier papers by Brunner, Paul, and Richter[8] and Paul, Brunner, and Richter[9] reviewed by Paul[10]). Nonclassical light fields with substantially sub-Poissonian statistics have great potential in optical communications, but to exploit this potential will require a detailed understanding of the change in photon statistics in switching and modulating.

In this paper we examine the photon statistics of light in a linear four-port coupler including dissipation and scattering using a straightforward Langevin quantum noise approach. First, we have calculated the photon distributions at the exit ports of a linear coupler, allowing both input ports to admit number-state or arbitrary-state inputs. In the case of a photon number-state input in one port and vacuum input into the second port, we show that an SU(2) coherent state of the kind described by Bužek and Quang[11] is produced. When a signal field enters one port and the vacuum enters the other port, the marginal photon distributions are shown to be equivalent to the photocount distributions relevant for imperfect photon detection of the signal field. The efficiency of the "detector" in this case is determined by the parameters of the coupler. On the other hand, when the vacuum is replaced by a strong coherent field, the output photon distributions are just those associated with homodyne detection of the signal field,[12] for both squeezed[13] and number-state signal inputs. Second, we have examined the effect of scattering coupling in the coupler on the squeezing and photon statistics of squeezed states. Scattering coupling is a phenomenon which occurs when imperfections in the coupler cause power to be scattered from the guided modes of one guide into those of the adjacent guide.[14] We model this in terms of a coupling of each mode to a common heat bath consisting of all the scattering modes of the guide. It is shown that the effect of scattering coupling equalizes the power in the two guides when the decay constants of the two are equal, thus prohibiting the switching of the fields entirely from one guide to the other. In consequence, any squeezing will be degraded, though not completely eliminated. Linear couplers can often be constructed with very low losses (for example, fiber-optic couplers). However, much attention has been paid to waveguides constructed from semiconductor materials.[15] Nonlinear multiple-quantum-well guides may well generate nonclassical light through their substantial nonlinearity but do possess non-negligible dissipative and scattering losses; were integrated systems using *linear* coupling to be employed as four-port devices in such semiconductors, the dissipative influences discussed here would become important. Similar considerations apply to any dissipative material.

The plan of this paper is as follows. In Sec. II we derive the coupled-mode equations for the coupler. In Secs. III and IV we examine the evolution of the photon statistical and squeezing properties of nonclassical fields in the coupler, paying particular attention to squeezed and number-state inputs. Finally, in Sec. V we turn our attention to the consequences of scattering coupling on the various properties of nonclassical state evolution in the coupler.

II. COUPLING BETWEEN TWO DIFFERENT WAVEGUIDES

The propagation of electromagnetic waves in a single optical waveguide can be solved exactly by application of the Maxwell equations.[16] This is not the case, however, in a two-guide structure, such as the linear directional coupler, where one must resort to perturbation methods. One such method is the so-called *coupled-mode theory,* which was first developed by Pierce[17] to treat the coupling between electron beam waves, and later extended to optical waveguides by Marcuse[14] and many others (see, e.g., Ref. 1 for references). In this approach one assumes that the presence of one guide introduces a small dielectric perturbation in the other guide. The electric (or magnetic) field of the composite structure may then be taken as a linear superposition of the unperturbed fields of each waveguide in isolation. If one then substitutes this into the Maxwell equations, one obtains two first-order differential equations in the slowly varying envelope approximation for the amplitudes of the fields in each guide, and these may be readily solved. One of the main predictions of the coupled-mode theory is the way in which energy can be transferred from one guide to the other in a controlled fashion, known as *directional* coupling.

Nonclassical states of light have received much attention over the past few years[13] mainly because of their potential application in high-performance communications networks[18–20] and the possibility of their use in detection of gravitational waves.[21] One important example of a nonclassical state of light is the squeezed state, characterized by a noise level in one quadrature phase that is less than that associated with the coherent state or the vacuum state.[13] In order to describe the propagation of nonclassical light in a coupler, we must quantize the relevant fields. We do this here in a phenomenological way, by treating the two guided modes of the coupler as a pair of linearly coupled harmonic oscillators.

A. Classical coupled-mode equations

An optical waveguide consists in its simplest form of a central core with a refractive index higher than the surrounding cladding material. A typical parameter used to characterize the waveguide is defined by[1,16]

$$V=ka(n_{\rm co}^2-n_{\rm cl}^2)^{1/2}\ , \tag{1}$$

where $k=2\pi/\lambda$, a is the radius of the core, λ is the waveguide of the light, and $n_{\rm cl}$ and $n_{\rm co}$ are the linear refractive indices of the cladding and the core. The parameter V determines the number of modes which the waveguide can support. For instance, if $V\lesssim 2.405$, then only one mode may propagate and the waveguide is said to be single moded. The modes which propagate unattenuated along the fiber are guided modes, as opposed to the radiation modes which radiate away. In a translationally invariant waveguide (here assumed to be along the z direction), the guided modes are expressible in the separable form[22]

$$E(x,y,z,t)=E_m(x,y)e^{i(\omega t-\beta_m z)}\ , \tag{2}$$

where $E_m(x,y)$ is the transverse mode pattern, β_m is the associated propagation constant, and ω is the frequency. We have assumed for simplicity that the fields are linearly polarized. For the linear directional coupler, we do not require explicit forms for the mode patterns. Each guided mode is a solution of the wave equation

$$\left[\nabla_t^2+\frac{\omega^2 n^2}{c^2}-\beta_m^2\right]E_m=0\ , \tag{3}$$

where $\nabla_t^2\equiv\partial^2/\partial x^2+\partial^2/\partial y^2$ is the transverse Laplacian operator. For the step-index profile waveguide, Eq. (3) must hold in each region of the guide and the fields matched at the core-cladding interface. It is easy to show from Eq. (3) the orthogonality of the guided modes to each other:[22]

$$\int\int E_m^*(x,y)E_n(x,y)dx\,dy=\frac{2\omega\mu_0}{|\beta_m|}\delta_{nm}\ , \tag{4}$$

where we have assumed the modes are normalized such that one unit of energy flows through the cross section of the waveguide.

A schematic arrangement of the coupler is shown in Fig. 1. Denoting the refractive index profiles of guides 1 and 2 by n_1 and n_2, respectively, the square of the refractive index profile of the composite structure may be written as[1]

$$n^2(x,y)=n_{\rm cl}^2+(n_1^2-n_{\rm cl}^2)+(n_2^2-n_{\rm cl}^2)\ . \tag{5}$$

The second and third terms in this expression are clearly zero outside the regions of guides 1 and 2. Each waveguide in isolation is assumed to support one guided mode E_i ($i=1,2$) with propagation constant β_i satisfying the wave equation

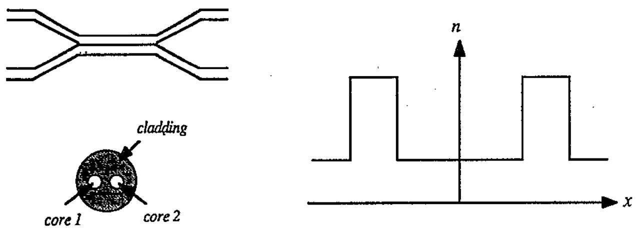

FIG. 1. Schematic illustration of a linear directional coupler, with two guides, shown with circular cross section for definiteness merging within a surrounding cladding material. The cross-sectional dependence of the refractive index n on position x is shown.

$$\left[\nabla_t^2+\frac{\omega^2 n_i^2}{c^2}-\beta_i^2\right]E_i=0, \quad i=1,2 . \tag{6}$$

In the framework of coupled-mode theory, the electric (or magnetic) field of the composite structure is assumed to be a linear superposition of the unperturbed fields:[22]

$$E_{\rm com}(x,y,z,t)=\alpha_1(z)E_1(x,y)e^{i(\omega t-\beta_1 z)}+\alpha_2(z)E_2(x,y)e^{i(\omega t-\beta_2 z)} , \tag{7}$$

where $\alpha_1(z)$ and $\alpha_2(z)$ are slowly varying functions of z. When the waveguides are placed sufficiently far apart, $\alpha_1(z)$ and $\alpha_2(z)$ are independent of z. Substituting Eq. (7) into the wave equation

$$\left[\nabla^2+\frac{\omega^2 n^2}{c^2}\right]E_{\rm com}=0 , \tag{8}$$

making the slowly varying amplitude approximation, and projecting out each mode amplitude, we find, after using the normalization condition (4),

$$\begin{aligned}\frac{d\alpha_1}{dz}&=-i\chi_{11}\alpha_1-i\chi_{12}\alpha_2 e^{i(\beta_1-\beta_2)z} ,\\ \frac{d\alpha_2}{dz}&=-i\chi_{22}\alpha_2-i\chi_{21}\alpha_1 e^{-i(\beta_1-\beta_2)z} ,\end{aligned} \tag{9}$$

where[22]

$$\begin{aligned}\chi_{ii}&=\frac{\omega\epsilon_0}{4}\int\int(n_i^2-n_{\rm cl}^2)E_j^*E_j\,dx\,dy, \quad i\neq j\\ \chi_{ij}&=\frac{\omega\epsilon_0}{4}\int\int(n_i^2-n_{\rm cl}^2)E_i^*E_j\,dx\,dy, \quad i\neq j .\end{aligned} \tag{10}$$

The terms χ_{ij} have the following meanings. The diagonal elements χ_{ii} are small corrections to the propagation constants β_i and arise due to the presence of the field of one guide in the other. The nondiagonal elements χ_{ij} $(i\neq j)$ are terms representing the coupling between the modes of the two guides and are much greater in magnitude than the diagonal elements.

By making the transformations

$$\begin{aligned}\beta_i&\to\tilde{\beta}_i=\beta_i+\chi_{ii} ,\\ \alpha_i&\to\tilde{\alpha}_i=\alpha_i e^{i\tilde{\beta}_i z} ,\end{aligned} \tag{11}$$

Eqs. (9) can be written in the more familiar form

$$\begin{aligned}\frac{d\tilde{\alpha}_1}{dz}&=-i\tilde{\beta}_1\tilde{\alpha}_1-i\chi_{12}\tilde{\alpha}_2 ,\\ \frac{d\tilde{\alpha}_2}{dz}&=-i\tilde{\beta}_2\tilde{\alpha}_2-i\chi_{21}\tilde{\alpha}_1 .\end{aligned} \tag{12}$$

When losses are present in the coupler, the propagation constants and coupling parameters are in general complex. Writing them in the form

$$\tilde{\beta}_i=\tilde{\beta}_i^R-i\gamma_i, \quad \chi_{ij}=\chi_{ij}^R-i\gamma_{ij} , \tag{13}$$

Eqs. (12) become

$$\begin{aligned}\frac{d\tilde{\alpha}_1}{dz}&=-i\tilde{\beta}_1^R\tilde{\alpha}_1-\gamma_1\tilde{\alpha}_1-i\chi_{12}^R\tilde{\alpha}_2-\gamma_{12}\tilde{\alpha}_2 ,\\ \frac{d\tilde{\alpha}_2}{dz}&=-i\tilde{\beta}_2^R\tilde{\alpha}_2-\gamma_2\tilde{\alpha}_2-i\chi_{21}^R\tilde{\alpha}_1-\gamma_{21}\tilde{\alpha}_1 ,\end{aligned} \tag{14}$$

where γ_1 and γ_2 are the amplitude extinction coefficients of modes 1 and 2, respectively. The last terms in Eqs. (14) represent the scattering of power from the guided mode of one guide into the guided mode of the adjacent guide. In the long-distance limit, they are responsible for equalizing the energies in the two guides[14] for equal dissipation in each mode. For purely *dissipative* losses rather than scattering between guides, they may be neglected.

B. Operator coupled-mode equations

Having established the standard classical coupled-mode equations incorporating dissipation and scattering, we now turn to a quantum-mechanical description of the same problem. We treat $\tilde{\alpha}_1$ and $\tilde{\alpha}_2$ as the amplitudes of two linearly coupled harmonic oscillators. These may be quantized in the standard way and dissipation incorporated by coupling each quantized oscillator to infinite heat baths of reservoir oscillators. The resultant quantum Langevin equations for the field mode annihilation operators a_i $(i=1,2)$ are closely analogous to the classical equations for the mode amplitudes [Eqs. (14)] and are given by[4]

$$\begin{aligned}\frac{da_1}{dz}&=-i\beta_1 a_1-\gamma_1 a_1-i\chi a_2+\Gamma_1 ,\\ \frac{da_2}{dz}&=-i\beta_2 a_2-\gamma_2 a_2-i\chi a_1+\Gamma_2 ,\end{aligned} \tag{15}$$

where we have assumed for simplicity that the coupling parameters are equal $(\chi_{12}=\chi_{21}=\chi)$, and that purely dissipative losses are considered. (We include mode coupling through scattering later.) The Langevin noise operators Γ_i $(i=1,2)$ are introduced to ensure that the correct commutation relations among the mode operators are maintained when losses are present; they arise naturally due to the coupling of each mode to a heat bath,[4] and are given by

$$\Gamma_i(z)=-i\sum_\lambda g_{i\lambda}e^{-i\beta_\lambda z}b_{i\lambda}(0), \quad i=1,2 \tag{16}$$

where $b_{i\lambda}$ are the bath annihilation operators and $g_{i\lambda}$ are the coupling constants.

The solutions to Eq. (15) are best expressed by defining the following quantities:

$$\bar{\beta}=\tfrac{1}{2}(\beta_1+\beta_2),\quad \Delta\beta=\tfrac{1}{2}(\beta_1-\beta_2)\,,$$
$$\bar{\gamma}=\tfrac{1}{2}(\gamma_1+\gamma_2),\quad \Delta\gamma=\tfrac{1}{2}(\gamma_1-\gamma_2)\,, \tag{17}$$
$$\tilde{\chi}=\sqrt{\chi^2+(\Delta\beta-i\Delta\gamma)^2}\,.$$

Then for a coupler of length L, we have

$$a_1(L)=u_1(L)a_1(0)+v_2(L)a_2(0)+\sum_\lambda[u_{1\lambda}(L)b_{1\lambda}+v_{2\lambda}(L)b_{2\lambda}(0)]\,,$$
$$a_2(L)=v_1(L)a_1(0)+u_2(L)a_2(0)+\sum_\lambda[v_{1\lambda}(L)b_{1\lambda}(0)+u_{2\lambda}(L)b_{2\lambda}(0)]\,, \tag{18}$$

where the coefficients $u_i(L),v_i(L)$ are given by

$$u_1(L)=\left[\cos\tilde{\chi}L-i\frac{\Delta\beta-i\Delta\gamma}{\tilde{\chi}}\sin\tilde{\chi}L\right]e^{-i\bar{\beta}L-\bar{\gamma}L}\,,$$
$$u_2(L)=\left[\cos\tilde{\chi}^*L+i\frac{\Delta\beta-i\Delta\gamma}{\tilde{\chi}^*}\sin\tilde{\chi}^*L\right]e^{-i\bar{\beta}L-\bar{\gamma}L}\,, \tag{19}$$
$$v_1(L)=-i\frac{\chi}{\tilde{\chi}^*}\sin\tilde{\chi}^*Le^{-i\bar{\beta}L-\bar{\gamma}L}\,,$$
$$v_2(L)=-i\frac{\chi}{\tilde{\chi}}\sin\tilde{\chi}Le^{-i\bar{\beta}L-\bar{\gamma}L}\,.$$

The bath variables $u_{i\lambda}$, etc. are given in the Appendix.

Losses in a coupler are quite often negligible.[23] In that case, Eqs. (18) reduce to the simpler forms

$$a_1(L)e^{i\bar{\beta}L}=u(L)a_1(0)+v(L)a_2(0)\,,$$
$$a_2(L)e^{i\bar{\beta}L}=v(L)a_1(0)+u^*(L)a_2(0)\,, \tag{20}$$

where

$$u(L)=\cos\tilde{\chi}L-i\frac{\Delta\beta}{\tilde{\chi}}\sin\tilde{\chi}L\,,$$
$$v(L)=-i\frac{\chi}{\tilde{\chi}}\sin\tilde{\chi}L\,,$$
$$\tilde{\chi}=\sqrt{\chi^2+\Delta\beta^2}=\tilde{\chi}^*\,. \tag{21}$$

Alternatively, Eqs. (20) may be rewritten in the compact form:

$$a_j(L)e^{i\bar{\beta}L}=\sum_k T_{jk}(L)a_k(0),\quad j,k=1,2 \tag{22}$$

where the elements $T_{jk}(L)$ are given by the unitary matrix

$$\tilde{T}(L)=\begin{bmatrix} u(L) & v(L)\\ v(L) & u^*(L)\end{bmatrix}\,, \tag{23}$$

$$\tilde{T}(L)\tilde{T}^{-1}(L)=1\,. \tag{24}$$

The matrix (23) acts in the space spanned by the operators $\{a_i,a_i^\dagger\}$ and corresponds to the evolution operator

$$T(L)=\exp[i\bar{\beta}-i\beta_1a_1^\dagger a_1-i\beta_2a_2^\dagger a_2-i\chi(a_1^\dagger a_2+a_2^\dagger a_1)]L\,. \tag{25}$$

Hence by similarity, we must also have that

$$T^\dagger(L)a_1(0)T(L)=u(L)a_1(0)+v(L)a_2(0)\,,$$
$$T^\dagger(L)a_2(0)T(L)=v(L)a_1(0)+u^*(L)a_2(0)\,. \tag{26}$$

The transformations (26) are immediately identified as the beam-splitter transformation.[6,24–27] Therefore the *lossless* coupler behaves in essentially the same way as a beam splitter, and results for the former should also apply for the latter.

III. PHOTON STATISTICS OF NONCLASSICAL LIGHT IN THE LINEAR DIRECTIONAL COUPLER

This section presents calculations for the photon distributions at the exit ports of a linear directional coupler for number-state inputs and for arbitrary-state inputs. Related calculations which cover some of these aspects have been carried out by Janszky, Sibilia, and Bertolotti,[3] and from the point of view of a quantum beam splitter, by Yurke, McCall, and Klauder,[24] Campos, Saleh, and Teich,[6] Prasad, Scully, and Martienssen,[25] Ou, Hong, and Mandel,[26] and Fearn and Loudon.[27]

A. Number-state inputs

Let us for the moment ignore all losses in the coupler. Then for an m_1- and an m_2-photon number state entering ports 1 and 2, respectively, the output state is given by

$$|\text{out}\rangle=T(L)|m_1\rangle_1|m_2\rangle_2=\frac{1}{\sqrt{m_1!m_2!}}T(L)a_1^{\dagger m_1}(0)a_2^{\dagger m_2}(0)|0\rangle_1|0\rangle_2\,, \tag{27}$$

which can be written in the form[25]

$$|\text{out}\rangle=\frac{1}{\sqrt{m_1!m_2!}}[ua_1^\dagger(0)+va_2^\dagger(0)]^{m_1}\times[va_1^\dagger(0)+u^*a_2^\dagger(0)]^{m_2}|0\rangle_1|0\rangle_2\,. \tag{28}$$

The associated joint photon distribution is obtained from a binomial expansion of Eq. (28) and using

$$P^{(m_1,m_2)}(n_1,n_2)=|{}_1\langle n_1|{}_2\langle n_2|\text{out}\rangle|^2\,. \tag{29}$$

The result is

$$P^{(m_1,m_2)}(n_1,n_2)=\frac{n_1!n_2!}{m_1!m_2!}s^{m_1+n_2}(1-s)^{m_2-n_2}\left[\sum_{r=\max(0,n_2-m_2)}^{\min(n_2,m_1)}(-1)^r\begin{bmatrix}m_1\\ r\end{bmatrix}\begin{bmatrix}m_2\\ n_2-r\end{bmatrix}s^{-r}(1-s)^r\right]^2,\quad m_1>m_2 \tag{30}$$

where $s=|u(L)|^2$. For $m_1<m_2$, we use the symmetry condition

$$P^{(m_1,m_2)}(n_1,n_2)=P^{(m_2,m_1)}(n_2,n_1) . \quad (31)$$

The marginal photon distributions are obtained by summing the joint photon distribution over n_1 or n_2:

$$P_1^{(m_1,m_2)}(n_1)=\sum_{n_2} P^{(m_1,m_2)}(n_1,n_2) ,$$
$$P_2^{(m_1,m_2)}(n_2)=\sum_{n_1} P^{(m_1,m_2)}(n_1,n_2) . \quad (32)$$

We consider below two special cases: (1) $m_1=m, m_2=0$ and (2) $m_1=m_2=m$.

1. $m_1=m, m_2=0$

The output state generated for this input configuration is the SU(2) coherent state, with its bosonic (or Schwinger) representation[11] given in the form described by Campos, Saleh, and Teich,[6]

$$|m,\tau\rangle=(1+|\tau|^2)^{-m/2}\sum_{r=0}^{m}\begin{bmatrix} m \\ r \end{bmatrix}^{1/2}\tau^r|r\rangle_1|m-r\rangle_2 , \quad (33)$$

where $\tau=u/v$. The fields emerging from the individual ports of the coupler are described by the reduced density matrices

$$\rho_1=\sum_{r=0}^{m}\begin{bmatrix} m \\ r \end{bmatrix}s^r(1-s)^{m-r}|r\rangle_{11}\langle r| ,$$
$$\rho_2=\sum_{r=0}^{m}\begin{bmatrix} m \\ r \end{bmatrix}(1-s)^r s^{m-r}|r\rangle_{22}\langle r| , \quad (34)$$

which are obtained by tracing Eq. (33) over the variables n_2 and n_1, respectively. From Eqs. (34) it is obvious that the marginal photon distributions for the individual modes are given by the binomial distributions

$$P_1(n)=\begin{bmatrix} m \\ n \end{bmatrix}s^n(1-s)^{m-n} ,$$
$$P_2(n)=\begin{bmatrix} m \\ n \end{bmatrix}(1-s)^n s^{m-n} , \quad (35)$$

with mean and variance given by

$$\langle n_1\rangle=sm, \quad \langle n_2\rangle=(1-s)m ,$$
$$\langle \Delta n_1^2\rangle=s(1-s)m, \quad \langle \Delta n_2^2\rangle=s(1-s)m . \quad (36)$$

A parameter used to characterize the deviation from Poissonian statistics is Mandel's Q parameter defined by[28]

$$Q=\frac{\langle \Delta n^2\rangle-\langle n\rangle}{\langle n\rangle} . \quad (37)$$

For the states (34), we have

$$Q_1=-s, \quad Q_2=-(1-s) . \quad (38)$$

As both quantities are negative, the photon statistics are sub-Poissonian in both modes. The anticorrelation between the output modes is described by the cross-correlation function, defined by

$$g^{(2)}\equiv\frac{\langle a_1^\dagger a_2^\dagger a_1 a_2\rangle}{\langle a_1^\dagger a_1\rangle\langle a_2^\dagger a_2\rangle} . \quad (39)$$

For the states (3), we find[11]

$$g^{(2)}=\frac{m-1}{m}\le 1 , \quad (40)$$

which is precisely the single-mode $g^{(2)}$ for a pure number state. As $g^{(2)}<1$, the two modes are clearly anticorrelated.

Dissipation modifies the marginal photon statistics from their values (32); the resultant Bernouilli sampling formulas for the marginal distributions become (see, e.g., Milburn and Walls[29])

$$P_1^{(m_1,m_2)}(n_1;\nu)=\sum_{l=n_1}^{\infty}\begin{bmatrix} l \\ n_1 \end{bmatrix}\nu^{n_1}(1-\nu)^{l-n_1}P_1^{(m_1,m_2)}(l) ,$$
$$P_2^{(m_1,m_2)}(n_2;\nu)=\sum_{l=n_2}^{\infty}\begin{bmatrix} l \\ n_2 \end{bmatrix}\nu^{n_2}(1-\nu)^{l-n_2}P_2^{(m_1,m_2)}(l) , \quad (41)$$

with $\nu=e^{-2\gamma L}$. For the binomial distributions (35), we have

$$P_1^{(m,0)}(n_1;\nu)=\sum_{l=n_1}^{m}\begin{bmatrix} l \\ n_1 \end{bmatrix}\begin{bmatrix} m \\ l \end{bmatrix}\nu^{n_1}(1-\nu)^{l-n_1}\times s^l(1-s)^{m-l} ,$$
$$P_2^{(m,0)}(n_2;\nu)=\sum_{l=n_2}^{m}\begin{bmatrix} l \\ n_2 \end{bmatrix}\begin{bmatrix} m \\ l \end{bmatrix}\nu^{n_2}(1-\nu)^{l-n_2}\times(1-s)^l s^{m-l} , \quad (42)$$

which can be summed in closed form to give

$$P_1^{(m,0)}(n_1;\nu)=\begin{bmatrix} m \\ n_1 \end{bmatrix}(\nu s)^{n_1}(1-\nu s)^{m-n_1} ,$$
$$P_2^{(m,0)}(n_2;\nu)=\begin{bmatrix} m \\ n_2 \end{bmatrix}(1-\nu s)^{n_2}(\nu s)^{m-n_2} . \quad (43)$$

The photon distributions thus remain binomial in the presence of dissipative losses. The above result agrees with that derived by Janszky, Sibilia, and Bertolotti[3] using quasiprobability methods.

2. $m_1=m_2=m$

This corresponds to the situation in which the same photon number state enters both ports of the coupler. The lack of phase in the initial states and the symmetric input means that the photon statistics of the fields emerging from both ports will be the same. The mean and variance of the photon number are given, respectively, by

$$\langle n_1\rangle=\langle n_2\rangle=m ,$$
$$\langle \Delta n_1^2\rangle=\langle \Delta n_2^2\rangle=2m(m+1)s(1-s) , \quad (44)$$

from which we obtain the Q parameter as

$$Q_1=Q_2=2(m+1)(1-s)s-1 . \quad (45)$$

The function (45) is plotted in Fig. 2. Sub-Poissonian photon statistics are found in the regions where

$$s>\tfrac{1}{2}+\tfrac{1}{2}\sqrt{(m-1)/(m+1)}\ ,\qquad s<\tfrac{1}{2}-\tfrac{1}{2}\sqrt{(m-1)/(m+1)}\ . \tag{46}$$

When $m\to\infty$, only super-Poissonian photon statistics appear at the output ports. Similarly, for the cross-correlation function, we obtain

$$g^{(2)}=1-2s(1-s)\left[\frac{m+1}{m}\right]. \tag{47}$$

As $g^{(2)}$ is less than unity in this case, the two modes are anticorrelated.

The marginal photon distributions are obtained using Eqs. (30) and (32). The results are plotted in Fig. 3. For $s=\frac{1}{2}$, the photons at either of the output ports appear only in pairs;[6,30] this feature is, however, extremely sensitive to any dissipation which may be present in the coupler, as demonstrated in Figs. 3(c) and 3(d).

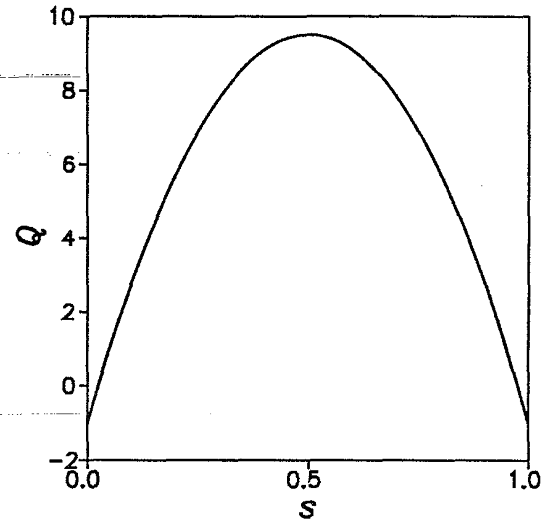

FIG. 2. Variation of the Q parameter of the output field as a function of the parameter s as given by Eq. (45) for the input state $|20\rangle_1|20\rangle_2$.

B. Arbitrary-state inputs

Consider now the case in which arbitrary states $|\xi_1\rangle_1$ and $|\xi_2\rangle_2$ enter ports 1 and 2 of the coupler, respectively. Suppose that we can expand $|\xi_1\rangle_1|\xi_2\rangle_2$ in terms of a photon number-state basis,

$$|\xi_1\rangle_1|\xi_2\rangle_2=\sum_{m_1,m_2}a_{m_1}b_{m_2}|m_1\rangle_1|m_2\rangle_2\ , \tag{48}$$

where a_{m_1} and b_{m_2} are in general complex coefficients and are assumed to satisfy the normalization conditions

$$\sum_{m_1}|a_{m_1}|^2=\sum_{m_2}|b_{m_2}|^2=1\ . \tag{49}$$

Then the output state will be given by

$$|\text{out}\rangle=T(L)|\xi_1\rangle_1|\xi_2\rangle_2=\sum_{m_1,m_2}a_{m_1}b_{m_2}T(L)|m_1\rangle_1|m_2\rangle_2\ , \tag{50}$$

from which we obtain the joint photon distribution

$$P^{(\xi_1,\xi_2)}(n_1,n_2)=\left|\sum_{k=0}^{n_1+n_2}a_kb_{n_1+n_2-k}T_{n_1n_2k\,n_1+n_2-k}\right|^2, \tag{51}$$

where the matrix elements $T_{n_1n_2m_1m_2}$ are given by

$$T_{n_1n_2m_1m_2}=\left[\frac{n_1!n_2!}{m_1!m_2!}\right]^{1/2}s^{(1/2)(m_1+n_2)}(1-s)^{(1/2)(m_2-n_2)}e^{i(m_1-n_2)\phi-i(m_2-n_2)\pi/2}\times\sum_{r=\max(0,n_2-m_2)}^{\min(n_2,m_1)}(-1)^r\begin{bmatrix}m_1\\ r\end{bmatrix}\begin{bmatrix}m_2\\ n_2-r\end{bmatrix}s^{-r}(1-s)^r,\quad m_1\ge m_2\ , \tag{52}$$

and the phase ϕ by

$$\phi=-\tan^{-1}\left[\frac{\Delta\beta}{\tilde{\chi}}\tan\tilde{\chi}L\right]. \tag{53}$$

The marginal photon distributions are obtained as before by summing the joint photon distribution over n_1 or n_2:

$$P_1^{(\xi_1,\xi_2)}(n_1)=\sum_{n_2}P^{(\xi_1,\xi_2)}(n_1,n_2)\ , \tag{54}$$

$$P_2^{(\xi_1,\xi_2)}(n_2)=\sum_{n_1}P^{(\xi_1,\xi_2)}(n_1,n_2)\ . \tag{55}$$

C. The coupler as a model for imperfect photon detection

When $|\xi_2\rangle_2$ is taken to be the vacuum state, the joint photon distribution (51) simplifies to

$$P^{(\xi_1,0)}(n_1,n_2)=P_1^{(\xi_1)}(n_1+n_2)P^{(n_1+n_2,0)}(n_1,n_2)\ , \tag{56}$$

where $P_1^{(\xi_1)}(n)$ is the photon distribution for the arbitrary state $|\xi_1\rangle_1$ and $P^{(n_1+n_2,0)}(n_1,n_2)$ is given by the binomial distribution

$$P^{(n_1+n_2,0)}(n_1,n_2)=\begin{bmatrix}n_1+n_2\\ n_1\end{bmatrix}s^{n_1}(1-s)^{n_2}\ . \tag{57}$$

Tracing out the n_2 variable from Eq. (56), we obtain the

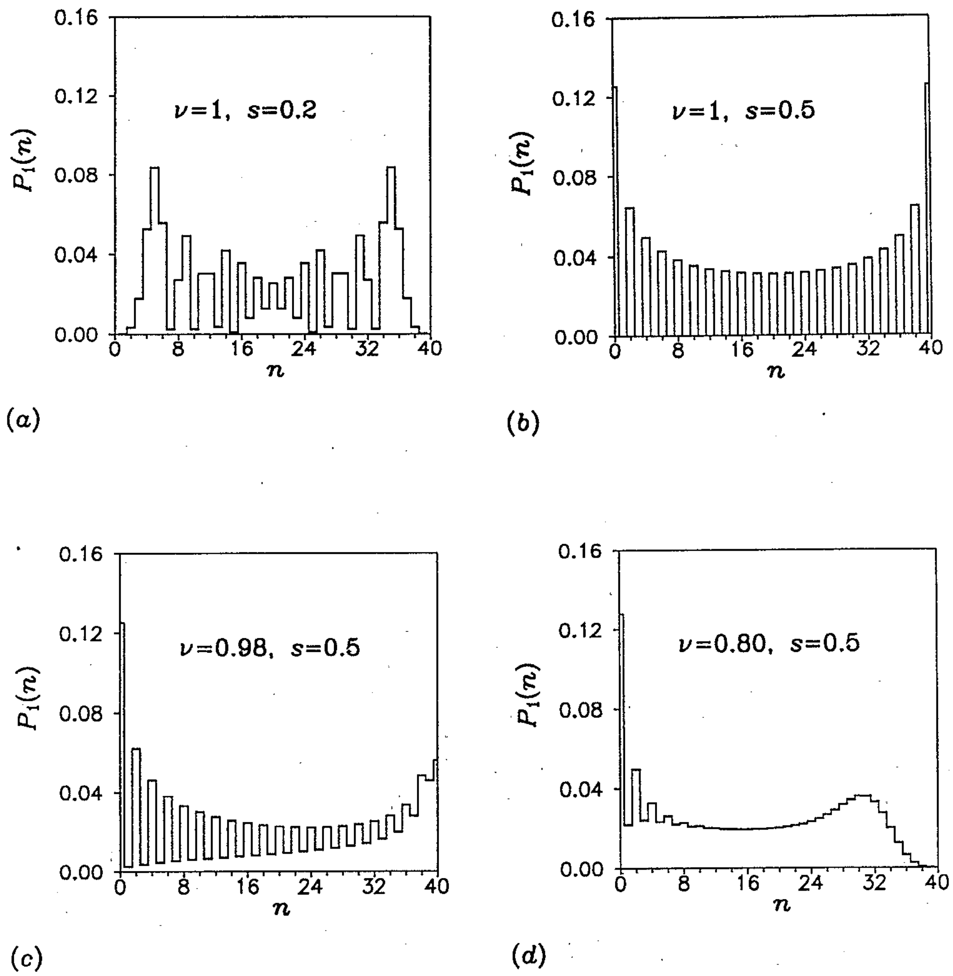

FIG. 3. Output marginal photon distributions $P_1(n)$ for the input state $|20\rangle_1|20\rangle_2$ as a function of photon number n, given by Eq. (32) for different values of the loss ν and the partition parameter s. For $s=0.5$, the output marginal photon distributions exhibit pairwise oscillations [plot (b)]. This feature is, however, extremely sensitive to any loss which may be present in the coupler [see plots (c) and (d) where the loss $\nu=\exp(-2\gamma L)$ is increased].

marginal photon distribution for output port 1 as

$$P_1^{(\xi_1,0)}(n_1)=\sum_{l=n_1}^{\infty}\begin{bmatrix} l \\ n_1\end{bmatrix} s^{n_1}(1-s)^{l-n_1}P_1^{(\xi_1)}(l)\ . \quad (58)$$

Equation (58) is the photocount distribution for imperfect photon detection[29] of the state $|\xi_1\rangle_1$ with efficiency s. The coupler is essentially a beam splitter, and splitting a field and mixing it with the vacuum entering from the unused port is fully equivalent to imperfect photon detection.[31] As an illustration, let $|\xi_1\rangle_1$ be a coherent state with Poissonian statistics

$$|\xi_1\rangle_1=|\alpha\rangle_1=e^{-|\alpha|^2/2}\sum_{n=0}^{\infty}\frac{\alpha^n}{\sqrt{n!}}|n\rangle_1\ . \quad (59)$$

The marginal photon distribution at output port 1 is obtained from Eq. (58) as

$$P_1^{(\alpha,0)}(n)=e^{-|\alpha'|^2}\frac{|\alpha'|^{2n}}{n!}\ , \quad (60)$$

where $\alpha'=u\alpha$. The photon distribution remains Poissonian but with a reduced mean. The initial photon distribution is recovered, however, when the coupler length L is such that $\tilde{\chi}L=\pi$.

D. The coupler as a model for homodyne detection

In homodyne detection, a signal field is mixed with a strong local coherent field and the beating between them measured by some photon detector.[12,13] The coupler carries out precisely this mixing process and may thus serve as a model for homodyne detection. The coherent field in this case would be launched into one guide and the much weaker signal field launched into the other, with

$$(1-s)|\alpha_L|^2 \gg s\langle n_{\text{signal}}\rangle\ , \quad (61)$$

where $\langle n_{\text{signal}}\rangle$ is the mean photon number in the signal field. Two types of homodyne detection schemes exist: ordinary homodyne detection (when $s\approx 1$) and balanced homodyne detection (when $s=\frac{1}{2}$). Both schemes are capable of probing the quadrature phases of nonclassical fields. In ordinary homodyne detection, one measures the marginal photon distributions. In balanced homodyne detection, on the other hand, one measures the difference photon distribution, given by

$$P_{\text{diff}}^{(\xi,\alpha_L)}(l)=\sum_n P^{(\xi,\alpha_L)}(n+l,n)\ , \qquad (62)$$

where $P^{(\xi,\alpha_L)}(n+l,n)$ is the joint photon distribution at the output ports of the coupler.

Consider ordinary homodyne detection of a k-photon number state. Using Eqs. (51), (54), and (55), we obtain, at the output ports, the marginal photon distributions

$$P_1^{(k,\alpha_L)}(n_1)=\sum_{n_2} P_2^{(\alpha_L)}(n_1+n_2-k) \times P^{(k,n_1+n_2-k)}(n_1,n_2)\theta(n_1+n_2-k)\ ,$$

$$P_2^{(k,\alpha_L)}(n_2)=\sum_{n_1} P_2^{(\alpha_L)}(n_1+n_2-k) \times P^{(k,n_1+n_2-k)}(n_1,n_2)\theta(n_1+n_2-k)\ , \qquad (63)$$

where $P_2^{(\alpha_L)}(n)$ is the photon distribution for the local oscillator field, $P^{(m_1,m_2)}(n_1,n_2)$ is given by Eq. (30), and $\theta(n)$ is the Heaviside step function. In ordinary homodyne detection, only the photon distribution $P_1^{(k,\alpha_L)}(n)$ will be measured. This function is plotted in Fig. 4 for $k=1$ and 2. The photon distributions are seen to closely resemble those for displaced number states.[32] This observation is readily explained by noting the fact that the coupler setup for ordinary homodyne detection effectively transforms the input state $|k\rangle_1|\alpha_L\rangle_2$ into the state $|v\alpha_L;k\rangle_1|u\alpha_L\rangle_2$, where $|\alpha;n\rangle$ is a displaced number state defined by

$$|\alpha;n\rangle\equiv D(\alpha)|n\rangle,\ \ D(\alpha)=e^{\alpha a^\dagger-\alpha^* a}\ , \qquad (64)$$

where $D(\alpha)$ is the Glauber displacement operator.[33]

Let us now suppose that the k-photon number state $|k\rangle_1$ enters port 1 and the coherent state $|\alpha\rangle_2$ of arbitrary strength enters port 2 of the coupler, respectively. In this case we can write the input state of the coupler as

$$|\text{in}\rangle=|k\rangle_1|\alpha\rangle_2=\frac{a_1^{\dagger k}(0)}{\sqrt{k!}}D_2(\alpha)|0\rangle_1|0\rangle_2\ . \qquad (65)$$

Using the evolution operator $T(L)$ we obtain for the output state of the coupler without making the strong field homodyne approximation the following expression:

$$|\text{out}\rangle=T(L)|\text{in}\rangle\ , \qquad (66)$$

or

$$|\text{out}\rangle=\exp[\alpha(va_1^\dagger+u^*a_2^\dagger)-\alpha^*(v^*a_1+ua_2)] \times\frac{1}{\sqrt{k!}}(ua_1^\dagger+va_2^\dagger)^k|0\rangle_1|0\rangle_2\ , \qquad (67)$$

where we have used the notation: $a_i(0)=a_i$; $v(L)=v$ and $u(L)=u$. We can rewrite the expression for the output state in the form

$$|\text{out}\rangle=\sum_{l=0}^{k}\begin{bmatrix}k\\ l\end{bmatrix}^{1/2} v^l u^{k-1}|v\alpha;k-l\rangle_1|u^*\alpha;l\rangle_2\ , \qquad (68)$$

from which we see that the linear directional coupler with the input state (65) can serve as a generator of mixtures of displaced number states in each of the output ports. It is easy to show that for high enough intensity of the coherent field and supposing that

$$|v|\ll|u| \qquad (69)$$

(i.e., $\tilde{\chi}L\approx\pi$), we obtain from Eq. (68) the relation for the output state of the coupler

$$|\text{out}\rangle\approx|v\alpha;k\rangle_1|u^*\alpha\rangle_2\ . \qquad (70)$$

In other words, we can say that under particular conditions (see above) the linear directional coupler can serve as a generator of displaced number states.

A squeezed coherent state is defined by[13]

$$|\alpha,\xi\rangle=D(\alpha)S(\xi)|0\rangle\ , \qquad (71)$$

where $S(\xi)$ is the squeezing operator

$$S(\xi)=\exp(\tfrac{1}{2}\xi^2a^{\dagger 2}-\tfrac{1}{2}\xi^*a^2)\ . \qquad (72)$$

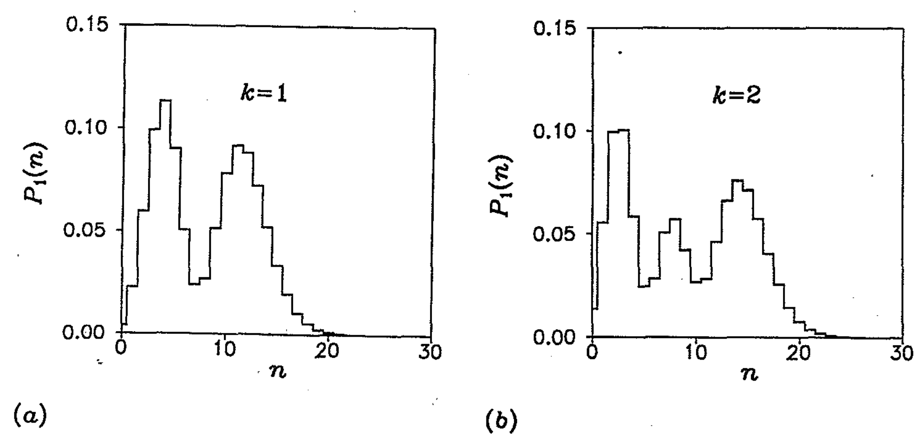

FIG. 4. Photon distribution $P_1(n)$ as a function of photon number n resulting from ordinary homodyning of (a) a one-photon number state, and (b) a two-photon number state. The amplitude of the local oscillator field was set to 7 and s to 0.85.

For the quadrature operators

$$X=\tfrac{1}{2}(a+a^\dagger),\quad Y=\frac{1}{2i}(a-a^\dagger)\,, \tag{73}$$

the squeezed state variances are

$$\langle \Delta X^2\rangle=\tfrac{1}{4}[\cos^2(\tfrac{1}{2}\theta)e^{-2r}+\sin^2(\tfrac{1}{2}\theta)e^{2r}]\,,$$
$$\langle \Delta Y^2\rangle=\tfrac{1}{4}[\cos^2(\tfrac{1}{2}\theta)e^{2r}+\sin^2(\tfrac{1}{2}\theta)e^{-2r}]\,, \tag{74}$$

where $\zeta=re^{i\theta}$. The squeezed state may be expanded in terms of a photon number state basis as[18]

$$|\alpha,\zeta\rangle=\sum_n b_n|n\rangle\,, \tag{75}$$

where the expansion coefficients b_n are given by

$$b_n=(n!\cosh r)^{-1/2}[\tfrac{1}{2}\exp(i\theta)\tanh r]^{n/2}$$
$$\times\exp\{-\tfrac{1}{2}[|\alpha|^2+\alpha^{*2}\exp(i\theta)\tanh r]\}$$
$$\times H_n\left[\frac{\alpha+\alpha^*\exp(i\theta)\tanh r}{(2\exp(i\theta)\tanh r)^{1/2}}\right]\,, \tag{76}$$

where H_n is a Hermite polynomial of order n.

Squeezed states are detected by employing either the ordinary or balanced homodyne detection schemes. In the former, the photon noise emerging from one output port is measured:

$$\langle \Delta n_1^2(L)\rangle \approx e^{-2\gamma L}\sin^2\chi L$$
$$\times\{1+e^{-2\gamma L}\cos^2\chi L[4\langle \Delta X_1^2(\psi)\rangle-1]\}|\alpha_L|^2, \tag{77}$$

where

$$\langle \Delta X_1^2(\psi)\rangle=\tfrac{1}{4}[\cos^2(\psi-\tfrac{1}{2}\theta)e^{-2r}+\sin^2(\psi-\tfrac{1}{2}\theta)e^{2r}]\,, \tag{78}$$

and $\psi=\phi_L-\pi/2$. The efficiency of the detector here is therefore governed by the dissipative loss in the coupler, and the transmittivity and reflectivity, by the coupling parameter. The shot noise due to the local oscillator [represented by the first term in Eq. (77)] may be eliminated by balance homodyning the signal. In that case the difference current corresponding to the operator

$$d^\dagger d=a_1^\dagger a_1-a_2^\dagger a_2 \tag{79}$$

is measured. The mean and variance of the operator (79) are easily shown to be given by

$$\langle n_d\rangle=2|\alpha_L|e^{-2\gamma L}\langle X_1(\psi)\rangle\,,$$
$$\langle \Delta n_d^2\rangle=|\alpha_L|^2e^{-2\gamma L}\{1+e^{-2\gamma L}[4\langle \Delta X_1^2(\psi)\rangle-1]\}\,, \tag{80}$$

where

$$X_1(\psi)=\tfrac{1}{2}[a_1^\dagger(0)e^{i\psi}+a_1(0)e^{-i\psi}]\,. \tag{81}$$

The corresponding difference photon distribution is obtained using Eq. (62), the result of which is displayed in the graphs of Fig. 5.

IV. QUADRATURE VARIANCES OF FIELDS IN THE LINEAR DIRECTIONAL COUPLER

The marginal quadrature variances at the output ports of the coupler are given by

$$\langle \Delta X_i^2(L)\rangle=\tfrac{1}{4}+\tfrac{1}{2}\mathrm{Re}[u_i^2(L)\langle \Delta a_i^2(0)\rangle$$
$$+v_{3-i}^2(L)\langle \Delta a_{3-i}^2(0)\rangle]$$
$$+\tfrac{1}{2}[|u_i(L)|^2\langle a_i^\dagger(0),a_i(0)\rangle$$
$$+|v_{3-i}(L)|^2\langle a_{3-i}^\dagger(0),a_{3-i}(0)\rangle]\,,$$
$$\langle \Delta Y_i^2(L)\rangle=\tfrac{1}{4}-\tfrac{1}{2}\mathrm{Re}[u_i^2(L)\langle \Delta a_i^2(0)\rangle$$
$$+v_{3-i}^2(L)\langle \Delta a_{3-i}^2(0)\rangle]$$
$$+\tfrac{1}{2}[|u_i(L)|^2\langle a_i^\dagger(0),a_i(0)\rangle$$
$$+|v_{3-i}(L)|^2\langle a_{3-i}^\dagger(0),a_{3-i}(0)\rangle]\,, \tag{82}$$

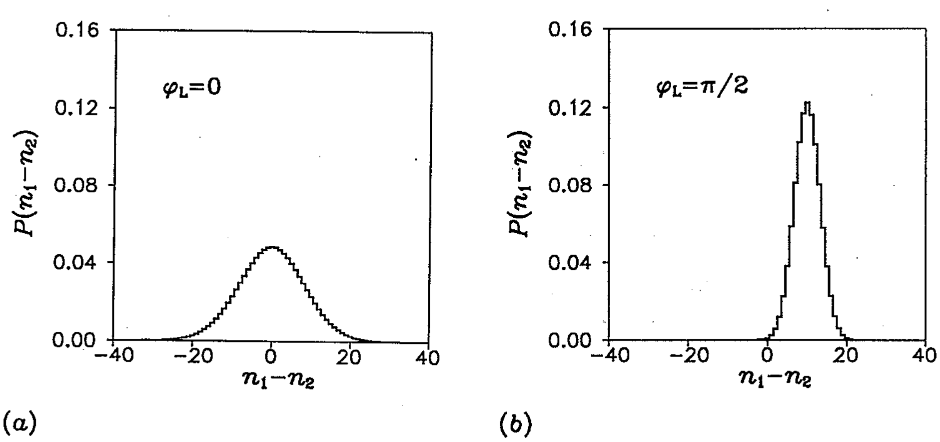

FIG. 5. Photon difference distribution $P(n_1-n_2)$ resulting from balanced homodyning of the squeezed state $|1,0.5\rangle$ from Eq. (62). The amplitude of the local oscillator field was set to 5, and the local oscillator phase chosen to be (a) $\phi_L=0$ and (b) $\phi_L=\pi/2$.

where $i=1,2$. When perfect phase matching is obtained and no losses are present, these reduce, in the interaction picture, to the simpler forms[2]

$$\langle \Delta X_i^2(L)\rangle = \langle \Delta X_i^2(0)\rangle \cos^2\chi L + \langle \Delta Y_{3-i}^2(0)\rangle \sin^2\chi L \;,$$
$$\langle \Delta Y_i^2(L)\rangle = \langle \Delta Y_i^2(0)\rangle \cos^2\chi L + \langle \Delta X_{3-i}^2(0)\rangle \sin^2\chi L \;. \qquad (83)$$

It is clear from these equations that fields can be switched entirely from one guide to the other without altering their quadrature variances.

In the presence of dissipation. Eqs. (83) are replaced by

$$\langle \Delta X_i^2(L)\rangle = \tfrac{1}{4}(1-e^{-2\gamma L}) + \langle \Delta X_i^2(0)\rangle e^{-2\gamma L}\cos^2\chi L + \langle \Delta Y_{3-i}^2(0)\rangle e^{-2\gamma L}\sin^2\chi L \;,$$
$$\langle \Delta Y_i^2(L)\rangle = \tfrac{1}{4}(1-e^{-2\gamma L}) + \langle \Delta Y_i^2(0)\rangle e^{-2\gamma L}\cos^2\chi L + \langle \Delta X_{3-i}^2(0)\rangle e^{-2\gamma L}\sin^2\chi L \;, \qquad (84)$$

where we have again assumed perfect phase matching. Figures 6(a) and 6(b) show the evolution of the variance in the X_1 quadrature for a squeezed state entering port 1 and the vacuum entering port 2 of the coupler. Dissipative losses lead to a degradation of squeezing, as seen in Fig. 6(b).

V. SCATTERING COUPLING IN THE LINEAR DIRECTIONAL COUPLER

Inhomogeneities in the dielectric medium composing the coupler can cause power to be scattered from the guided modes of one guide into those of the adjacent guide,[14] and prevents complete transference of power from one guide to the other. Scattering coupling may be modeled quantum mechanically by coupling each mode to a common set of scattering modes. The Hamiltonian is then of the form

$$H = H_0 + H_I + H_{\text{bath}} \;, \qquad (85)$$

where

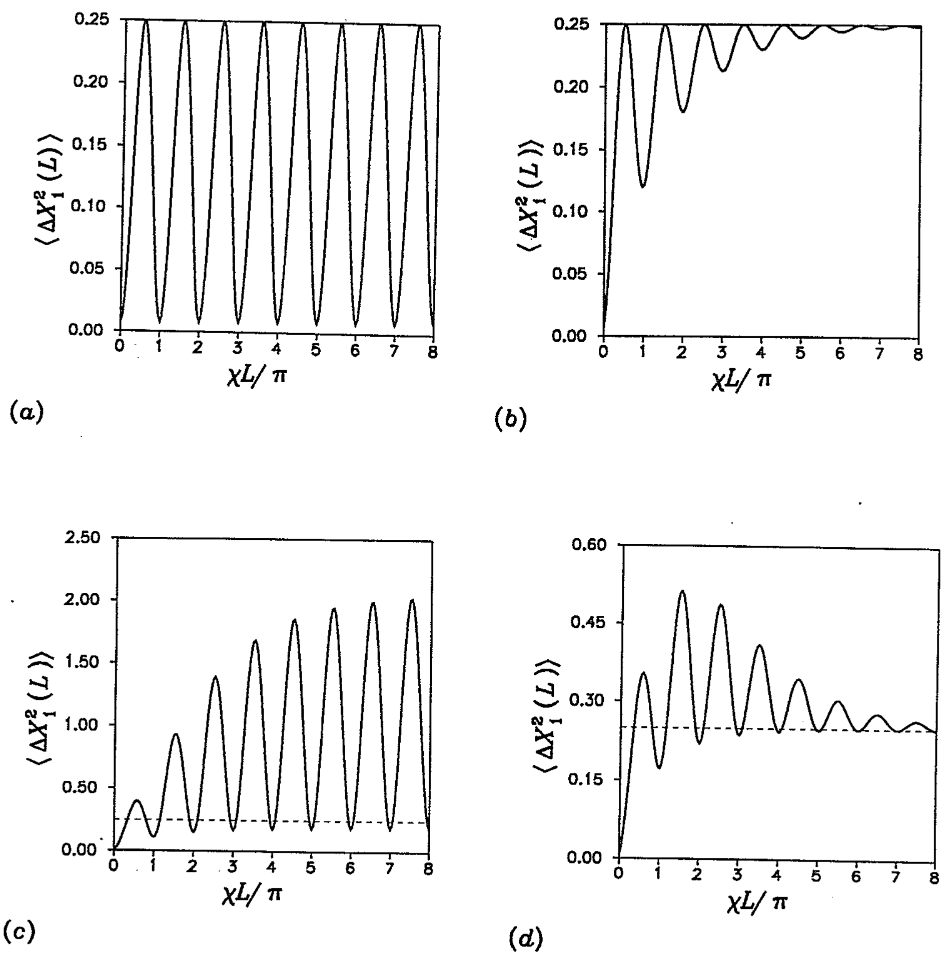

FIG. 6. Quadrature variance $\langle \Delta X_1^2(L)\rangle$ as a function of coupler length for a squeezed state input in the presence of (a) zero losses, (b) purely dissipative losses ($\gamma_d=0.1\chi$), (c) scattering losses ($\gamma_s=0.1\chi$), and (d) both dissipative and scattering losses ($\gamma_d=2\gamma_s=0.2\chi$).

$$H_0=\hbar\omega(a_1^\dagger a_1+a_2^\dagger a_2)+\hbar\sum_\lambda \omega_\lambda b_\lambda^\dagger b_\lambda \,,$$
$$H_I=\hbar v^{-1}\chi(a_1^\dagger a_2+a_2^\dagger a_1)\,, \tag{86}$$
$$H_{\rm bath}=\hbar v^{-1}\sum_\lambda [g_\lambda(a_1^\dagger-a_2^\dagger)b_\lambda+g_\lambda^* b_\lambda^\dagger(a_1-a_2)]\,,$$

and we have assumed for simplicity that the modes are sufficiently close in frequency to see the bath in an identical way, and propagate with the same group velocity v. Quantum Langevin equations for the field mode annihilation operators are derived by assuming the bath is broad band and allows the Born-Markov approximation to be used.[4] The result is given by

$$\frac{da_1}{dz}=-i\beta a_1-i\chi a_2-\gamma_s(a_1-a_2)+\Gamma\,,$$
$$\frac{da_2}{dz}=-i\beta a_2-i\chi a_1-\gamma_s(a_2-a_1)+\Gamma\,, \tag{87}$$

where we have replaced t by z/v. The scattering rate parameter γ_s is given by

$$\gamma_s=v^{-2}\pi|g(\omega)|^2\rho(\omega) \tag{88}$$

[$\rho(\omega)$ is the density of states for the bath oscillators], and the Langevin noise operator Γ by

$$\Gamma(z)=-i\sum_\lambda g_\lambda b_\lambda(0)e^{-i\beta_\lambda z}\,. \tag{89}$$

The solution to Eqs. (87) is as follows:

$$a_1(L)=u'(L)a_1(0)+v'(L)a_2(0)+\sum_\lambda u_\lambda(L)b_\lambda(0)\,,$$
$$a_2(L)=u'(L)a_2(0)+v'(L)a_1(0)+\sum_\lambda u_\lambda(L)b_\lambda(0)\,, \tag{90}$$

where

$$u'(L)=\tfrac{1}{2}e^{-i\beta L}(e^{i\chi L-2\gamma_s L}+e^{-i\chi L})\,,$$
$$v'(L)=-\tfrac{1}{2}e^{-i\beta L}(e^{i\chi L-2\gamma_s L}-e^{-i\chi L})\,,$$
$$u_\lambda(L)=g_\lambda e^{-i\beta_\lambda L}\left[\frac{1-e^{i(\beta_\lambda-\beta+\chi)L-2\gamma_s L}}{\beta_\lambda-\beta+\chi+2i\gamma_s}\right]\,. \tag{91}$$

We obtain, on tracing over the zero-temperature heat-bath variables, the symmetric and antisymmetric combination of mode "reduced" operators of the composite two-guide structure:

$$a_+(L)\equiv a_1(L)+a_2(L)=a_+(0)e^{-i(\beta+\chi)L}\,,$$
$$a_-(L)\equiv a_1(L)-a_2(L)=a_-(0)e^{-i(\beta-\chi)L-2\gamma_s L}\,. \tag{92}$$

Scattering coupling attenuates the antisymmetric mode, whereas the symmetric mode propagates freely. This is found indeed to be the case in fiber couplers with sufficiently small waveguide parameters.[34]

The mean mode energy in each guide is given by

$$\langle a_i^\dagger(L)a_i(L)\rangle=|u'(L)|^2\langle a_i^\dagger(0)a_i(0)\rangle$$
$$+|v'(L)|^2\langle a_{3-i}^\dagger(0)a_{3-i}(0)\rangle$$
$$+2\,{\rm Re}u'^*(L)v'(L)\langle a_i^\dagger(0)a_{3-i}(0)\rangle\,,$$
$$i=1,2\,. \tag{93}$$

If the field is initially launched into guide 1 with a vacuum input for guide 2, then from Eq. (93), we find

$$\langle a_1^\dagger(L)a_1(L)\rangle=\tfrac{1}{4}(1+e^{-4\gamma_s L}+2e^{-2\gamma_s L}\cos2\chi L)\times\langle a_1^\dagger(0)a_1(0)\rangle\,,$$
$$\langle a_2^\dagger(L)a_2(L)\rangle=\tfrac{1}{4}(1+e^{-4\gamma_s L}-2e^{-2\gamma_s L}\cos2\chi L)\times\langle a_1^\dagger(0)a_1(0)\rangle\,. \tag{94}$$

A plot of the mean mode energy in guide 1 as a function of coupler length is shown in Fig. 7. Initially there is some interchange of energy between the two guides of the coupler. However, in the long-distance limit, the mean mode energies in each guide equalize and approach the asymptotic value

$$\langle a_1^\dagger(L)a_1(L)\rangle_{L\to\infty}=\langle a_2^\dagger(L)a_2(L)\rangle_{L\to\infty}$$
$$=\tfrac{1}{4}\langle a_1^\dagger(0)a_1(0)\rangle\,. \tag{95}$$

Therefore, in the long-distance limit, half of the initial energy is radiated away and half redistributed in the guided modes of the coupler.

As an illustration of the effect of scattering coupling on the evolution of the quadrature variances, we consider a squeezed coherent state $|\alpha,\xi\rangle$ input entering port 1 of the coupler and vacuum input into port 2. Then for the output quadrature variance, we obtain

$$\langle\Delta X_1^2(L)\rangle=A(L)+\tfrac{1}{4}[B(L)e^{-2r}+C(L)e^{2r}]\,, \tag{96}$$

where

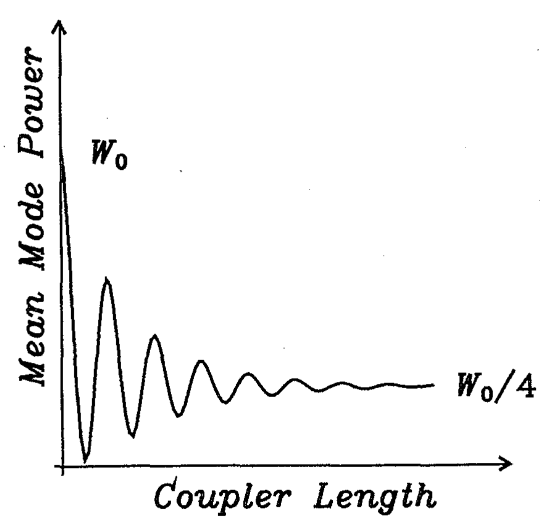

FIG. 7. Mean mode power as a function of coupler length (both in arbitrary units) in the presence of scattering losses.

$$A(L)=\tfrac{3}{16}-\tfrac{1}{8}e^{-2\gamma_s L}\cos 2\chi L-\tfrac{1}{16}e^{-4\gamma_s L},$$
$$B(L)=\tfrac{1}{4}\{\cos[(\beta+\chi)L-\tfrac{1}{2}\theta]+e^{-2\gamma_s L}\cos[(\beta-\chi)L-\tfrac{1}{2}\theta]\}^2, \quad (97)$$
$$C(L)=\tfrac{1}{4}\{\sin[(\beta+\chi)L-\tfrac{1}{2}\theta]+e^{-2\gamma_s L}\sin[(\beta-\chi)L-\tfrac{1}{2}\theta]\}^2 .$$

Clearly apparent in Eq. (97) is the decay of components at the antisymmetric mode frequency due to scattering coupling. It is precisely this decay which causes the degradation of squeezing, as observed in Fig. 6(c).

In the long-distance limit, the quadrature variance (96) approaches the value

$$\langle \Delta X_1^2(L)\rangle_{L\to\infty}\to\tfrac{3}{16}+\tfrac{1}{16}\{\cos^2[(\beta+\chi)L-\tfrac{1}{2}\theta]e^{-2r}+\sin^2[(\beta+\chi)L-\tfrac{1}{2}\theta]e^{2r}\} . \quad (98)$$

Therefore, in the event of an infinitely squeezed input, the maximum squeezing achievable in the long-distance limit is just 25% below the shot noise level. In view of this, one must be careful to avoid scattering coupling in communications systems using squeezed states.

Dissipative losses are always present in the coupler, and are modeled by coupling each mode to its own heat bath. In that case Eq. (96) is replaced by

$$\langle \Delta X_1^2(L)\rangle=A'(L)+\tfrac{1}{4}[B'(L)e^{-2r}+C'(L)e^{2r}], \quad (99)$$

where

$$A'(L)=\tfrac{1}{4}(1-e^{-2\gamma_d L})+e^{-2\gamma_d L}A(L),$$
$$B'(L)=e^{-2\gamma_d L}B(L), \quad (100)$$
$$C'(L)=e^{-2\gamma_d L}C(L),$$

and γ_d is the amplitude extinction coefficient of each mode. The function (99) is plotted in Fig. 6(d).

The mean and variance of the photon number of the field emerging from guide 1 for the same input as before and in the presence of scattering losses are given, respectively, by

$$\langle n_1(L)\rangle=|u'(L)|^2\langle n_1(0)\rangle_{sq},$$
$$\langle \Delta n_1^2(L)\rangle=|u'(L)|^4\langle \Delta n_1^2(0)\rangle_{sq}+|u'(L)|^2|v(L)|^2\langle n_1(0)\rangle_{sq}, \quad (101)$$

and hence for the Q parameter, we have

$$Q_1(L)=|u'(L)|^2\left[\frac{\langle \Delta n_1^2(0)\rangle_{sq}}{\langle n_1(0)\rangle_{sq}}-1\right]-\tfrac{1}{2}(1-e^{-4\gamma_s L}), \quad (102)$$

where $\langle\ \rangle_{sq}$ denotes an average over a squeezed state. Sub-Poisson photon statistics will therefore be always obtained if the initial squeezed field statistics is also sub-Poissonian.

In the homodyne detection of a squeezed state, one replaces the vacuum entering the unused port of the coupler by a strong local oscillator field. The variance of the photon number of the field emerging from guide 1 will then be given by

$$\langle \Delta n_1^2(L)\rangle\approx|\alpha_L|^2\{F(L)+\tfrac{1}{4}[G(L)e^{-2r}+H(L)e^{2r}]\}, \quad (103)$$

where

$$F(L)=\tfrac{1}{4}(1+e^{-4\gamma_s L}-2e^{-2\gamma_s L}\cos 2\chi L)-\tfrac{1}{16}[(1+e^{-4\gamma_s L})^2-4e^{-4\gamma_s L}\cos^2 2\chi L]+\tfrac{1}{16}e^{-2\gamma_s L}(1-e^{-4\gamma_s L})\times\sin 2\chi L\,\sin 2(\phi_L-\tfrac{1}{2}\theta)\sinh 2r,$$
$$G(L)=\tfrac{1}{4}[\cos^2(\phi_L-\tfrac{1}{2}\theta)(1-e^{-4\gamma_s L})^2+4e^{-4\gamma_s L}\sin^2 2\chi L\,\sin^2(\phi_L-\tfrac{1}{2}\theta)], \quad (104)$$
$$H(L)=\tfrac{1}{4}[\sin^2(\phi_L-\tfrac{1}{2}\theta)(1-e^{-4\gamma_s L})^2+4e^{-4\gamma_s L}\sin^2 2\chi L\,\cos^2(\phi_L-\tfrac{1}{2}\theta)] .$$

In the presence of scattering coupling therefore no simple relation exists between $\langle \Delta n_1^2(L)\rangle$ and $\langle \Delta X_1^2(\psi)\rangle$. Therefore one cannot determine the squeezing in the input field *simply* from the photon statistics of the output field. However, in the long-distance limit, a simple relation does exist and is given by

$$\langle \Delta n_1^2(L)\rangle=|\alpha_L|^2\langle \Delta X_1^2(\psi)\rangle_{L\to\infty}, \quad (105)$$

where

$$\langle \Delta X_1^2(\psi)\rangle_{L\to\infty}=\tfrac{3}{16}+\tfrac{1}{16}[\cos^2(\psi-\tfrac{1}{2}\theta)e^{-2r}+\sin^2(\psi-\tfrac{1}{2}\theta)e^{2r}], \quad (106)$$

and $\psi=\alpha_L-\pi/2$. The corresponding Q parameter is

$$Q_1(L)_{L\to\infty}=\langle \Delta X_1^2(\psi)\rangle-\tfrac{1}{4} . \quad (107)$$

Therefore, in the presence of scattering coupling, squeezing in the input field may still be detected provided the coupler length is sufficiently large, and is revealed by sub-Poissonian photon statistics in the output field.

In the presence of dissipative losses and scattering, Eq. (103) is to be replaced by the more complicated expression

$$\langle \Delta n_1^2(L)\rangle=|\alpha_L|^2\{F'(L)+\tfrac{1}{4}[G'(L)e^{-2r}+H'(L)e^{2r}]\}, \quad (108)$$

where

$$F'(L)=\tfrac{1}{4}(1+e^{-4\gamma_d L}-2e^{-2\gamma_d L}\cos 2\chi L)\times(1-e^{-2\gamma_d L})e^{-2\gamma_d L}+e^{-4\gamma_d L}F(L)\,,$$
$$G'(L)=e^{-4\gamma_d L}G(L)\,, \tag{109}$$
$$H'(L)=e^{-2\gamma_d L}H(L)\,.$$

VI. CONCLUSIONS

We have studied the photon statistics of nonclassical fields in a linear directional coupler. Using the solutions to the operator equations of motion, we have calculated the photon distributions at the output ports of the coupler for number-state inputs and for arbitrary-state inputs. We have demonstrated that when a number state enters one port of the coupler and the vacuum enters the other port, an SU(2) coherent state is generated at the output ports. Each mode of this SU(2) coherent state was shown to have a photon distribution given by the binomial distribution. We then demonstrated that when the same number state enters both ports of the coupler, the probability of finding an odd number of photons at either of the output ports vanishes for some choice of the coupler length. Generalizing to the case in which an arbitrary state enters one port and the vacuum enters the other port, we then found that coupler essentially behaves as an imperfect photon detector with efficiency governed by the coupler parameters. On the other hand, we found, that by replacing the vacuum entering the unused port with a strong local coherent field, the coupler behaves essentially as a homodyne detector. Dissipative losses within the coupler determine the efficiency of the detector. Calculations for the photon distribution associated with ordinary homodyne detection of a number state and the difference photon distribution associated with balanced homodyne detection of a squeezed state were presented. In the former we showed that displaced photon number statistics are produced and in the latter the phase sensitivity of the photon distribution to the local oscillator phase.

Finally, we examined the effect of scattering coupling in the coupler. We showed that scattering coupling tends to equalize the energy in each guide. As a consequence, the evolution of the quadrature variances and photon statistics of squeezed states of light follow a very complicated pattern. In the presence of scattering coupling, the coupler does not behave either like an imperfect photon detector or a homodyne detector.

ACKNOWLEDGMENTS

We would like to thank S. Phoenix for useful discussions. This work was supported in part by the United Kindgom Science and Engineering Research Council.

APPENDIX: COUPLED OPERATOR SOLUTIONS

The solution to the coupled-mode operator equations of motion

$$\frac{da_1}{dz}=-i\beta_1 a_1-\gamma_1 a_1-i\chi a_2+\Gamma_1\,,$$
$$\frac{da_2}{dz}=-i\beta_2 a_2-\gamma_2 a_2-i\chi a_1+\Gamma_2$$

is obtained using Laplace transforms. The result is given by

$$a_1(L)=u_1(L)a_1(0)+v_2(L)a_2(0)+\sum_\lambda[u_{1\lambda}(L)b_{1\lambda}(0)+v_{2\lambda}(L)b_{2\lambda}(0)]\,,$$
$$a_2(L)=v_1(L)a_1(0)+u_2(L)a_2(0)+\sum_\lambda[v_{1\lambda}(L)b_{1\lambda}(0)+u_{2\lambda}(L)b_{2\lambda}(0)]\,,$$

where

$$u_1(L)=\left[\cos\tilde{\chi}L-i\frac{\Delta\beta-i\Delta\gamma}{\tilde{\chi}}\sin\tilde{\chi}L\right]e^{-i\bar{\beta}L-\bar{\gamma}L},\quad u_2(L)=\left[\cos\tilde{\chi}^*L+i\frac{\Delta\beta-i\Delta\gamma}{\tilde{\chi}^*}\sin\tilde{\chi}^*L\right]e^{-i\bar{\beta}L-\bar{\gamma}L}\,,$$

$$v_1(L)=-i\frac{\chi}{\tilde{\chi}^*}\sin\tilde{\chi}^*Le^{-i\bar{\beta}L-\bar{\gamma}L},\quad v_2(L)=-i\frac{\chi}{\tilde{\chi}}\sin\tilde{\chi}Le^{-i\bar{\beta}L-\bar{\gamma}L}\,,$$

$$u_{1\lambda}(L)=g_{1\lambda}e^{-i\beta_\lambda L}\left[\frac{\beta_\lambda-\beta_2+i\gamma_2}{(\beta_\lambda-\bar{\beta}^{(+)}-i\bar{\gamma})(\beta_\lambda-\bar{\beta}^{(-)}-i\bar{\gamma})}-\frac{1}{2}\frac{\tilde{\chi}-\Delta\beta+i\Delta\gamma}{\tilde{\chi}(\beta_\lambda-\bar{\beta}^{(-)}-i\bar{\gamma})}e^{i(\beta_\lambda-\bar{\beta}^{(-)}-i\bar{\gamma})L}\right.$$
$$\left.+\frac{1}{2}\frac{\tilde{\chi}+\Delta\beta-i\Delta\gamma}{\tilde{\chi}(\beta_\lambda-\bar{\beta}^{(+)}-i\bar{\gamma})}e^{i(\beta_\lambda-\bar{\beta}^{(+)}-i\bar{\gamma})L}\right]\,,$$

$$u_{2\lambda}(L)=g_{2\lambda}e^{-i\beta_\lambda L}\left[\frac{\beta_\lambda-\beta_1+i\gamma_1}{(\beta_\lambda-\bar{\beta}^{(+)*}-i\bar{\gamma})(\beta_\lambda-\bar{\beta}^{(-)*}-i\bar{\gamma})}-\frac{1}{2}\frac{\tilde{\chi}^*+\Delta\beta-i\Delta\gamma}{\tilde{\chi}^*(\beta_\lambda-\bar{\beta}^{(-)*}-i\bar{\gamma})}e^{i(\beta_\lambda-\bar{\beta}^{(-)*}-i\bar{\gamma})L}\right.$$
$$\left.+\frac{1}{2}\frac{\tilde{\chi}^*-\Delta\beta+i\Delta\gamma}{\tilde{\chi}^*(\beta_\lambda-\bar{\beta}^{(+)*}-i\bar{\gamma})}e^{i(\beta_\lambda-\bar{\beta}^{(+)*}-i\bar{\gamma})L}\right]\,,$$

$$v_{1\lambda}(L)=g_{1\lambda}e^{-i\beta_\lambda L}\left[\frac{\chi}{(\beta_\lambda-\bar{\beta}^{(+)*}-i\bar{\gamma})(\beta_\lambda-\bar{\beta}^{(-)*}-i\bar{\gamma})}+\frac{1}{2}\frac{\chi}{\tilde{\chi}^*(\beta_\lambda-\bar{\beta}^{(-)*}-i\bar{\gamma})}e^{i(\beta_\lambda-\bar{\beta}^{(-)*}-i\bar{\gamma})L}-\frac{1}{2}\frac{\chi}{\tilde{\chi}^*(\beta_\lambda-\bar{\beta}^{(+)*}-i\bar{\gamma})}e^{i(\beta_\lambda-\bar{\beta}^{(+)*}-i\bar{\gamma})L}\right]$$

$$v_{2\lambda}(L)=g_{2\lambda}e^{-i\beta_\lambda L}\left[\frac{\chi}{(\beta_\lambda-\bar{\beta}^{(+)}-i\bar{\gamma})(\beta_\lambda-\bar{\beta}^{(-)}-i\bar{\gamma})}+\frac{1}{2}\frac{\chi}{\tilde{\chi}(\beta_\lambda-\bar{\beta}^{(-)}-i\bar{\gamma})}e^{i(\beta_\lambda-\bar{\beta}^{(-)}-i\bar{\gamma})L}-\frac{1}{2}\frac{\chi}{\tilde{\chi}(\beta_\lambda-\bar{\beta}^{(+)}-i\bar{\gamma})}e^{i(\beta_\lambda-\bar{\beta}^{(+)}-i\bar{\gamma})L}\right],$$

and

$$\bar{\beta}=\tfrac{1}{2}(\beta_1+\beta_2),\quad \Delta\beta=\tfrac{1}{2}(\beta_1-\beta_2),\quad \bar{\gamma}=\tfrac{1}{2}(\gamma_1+\gamma_2),\quad \Delta\gamma=\tfrac{1}{2}(\gamma_1-\gamma_2),$$

$$\bar{\beta}^{(+)}=\bar{\beta}+\tilde{\chi},\quad \bar{\beta}^{(-)}=\bar{\beta}-\tilde{\chi},\quad \tilde{\chi}=\sqrt{\chi^2+(\Delta\beta-i\Delta\gamma)^2}\,.$$

---

*Permanent address: Institute of Physics, Slovak Academy of Sciences, Dúbravská cesta 9, 842 28 Bratislava, Czechoslovakia.

[1]See, e.g., D. Marcuse, *Light Transmission Optics* (Van Nostrand Reinhold, New York, 1982).

[2]J. Janszky, C. Sibilia, and M. Bertolotti, J. Mod. Opt. **35**, 1757 (1988).

[3]J. Janszky, C. Sibilia, and M. Bertolotti, J. Mod. Opt. (to be published).

[4]See, e.g., W. H. Louisell, *Quantum Statistical Properties of Radiation* (Wiley, New York, 1973).

[5]By this we mean that the field-mode density matrix leads to binomial counting statistics, which should be distinguished from a pure binomial field state investigated by B. E. A. Saleh and M. C. Teich, Opt. Acta **32**, 345 (1985).

[6]R. A. Campos, B. E. A. Saleh, and M. C. Teich, Phys. Rev. A **40**, 1371 (1989).

[7]R. Loudon, Rep. Prog. Phys. **43**, 913 (1980).

[8]W. H. Brunner, H. Paul, and G. Richter, Ann. Phys. (Leipzig) **15**, 17 (1965).

[9]H. Paul, W. H. Brunner, and G. Richter, Ann. Phys. (Leipzig) **17**, 262 (1966).

[10]H. Paul, Rev. Mod. Phys. **54**, 1061 (1982).

[11]V. Bužek and T. Quang, J. Opt. Soc. Am. B **6**, 2448 (1989), and references therein.

[12]H. P. Yuen and V. W. S. Chan, Opt. Lett. **8**, 177 (1983).

[13]See, e.g., the reviews by D. F. Walls, Nature (London) **306**, 141 (1983); R. Loudon and P. L. Knight, J. Mod. Opt. **34**, 709 (1987).

[14]D. Marcuse, Bell System Tech. J. **50**, 1791 (1971); **50**, 1817 (1971).

[15]P. N. Butcher and D. Cotter, *The Elements of Nonlinear Optics* (Cambridge University Press, Cambridge, 1990).

[16]See, e.g., A. W. Synder and J. D. Love, *Optical Waveguide Theory* (Chapman and Hall, London, 1983).

[17]J. R. Pierce, J. Appl. Phys. **25**, 179 (1954).

[18]H. P. Yuen, Phys. Rev. A **13**, 2226 (1976).

[19]Y. Yamamoto and H. A. Haus, Rev. Mod. Phys. **58**, 1001 (1986).

[20]R. E. Slusher and B. Yurke, J. Light Wave Tech. **8**, 466 (1990).

[21]C. M. Caves, Phys. Rev. D **23**, 1693 (1981).

[22]D. Yeh, *Optical Waves in Layered Media* (Wiley, New York, 1989).

[23]Typical losses in fiber couplers are of the order of 1 dB [see, e.g., G. P. Agrawal, *Nonlinear Fiber Optics* (Academic, San Diego, 1989)].

[24]B. Yurke, S. L. McCall, and J. R. Klauder, Phys. Rev. A **33**, 4033 (1986).

[25]S. Prasad, M. O. Scully, and W. Martienssen, Opt. Commun. **62**, 139 (1987).

[26]Z. Ou, C. K. Hong, and L. Mandel, Opt. Commun. **63**, 118 (1987).

[27]H. Fearn and R. Loudon, Opt. Commun. **64**, 485 (1987).

[28]L. Mandel, Opt. Lett. **4**, 305 (1979).

[29]G. J. Milburn and D. F. Walls, Phys. Rev. A **38**, 1087 (1989); see also B. R. Mollow, Phys. Rev. **168**, 1896 (1968); M. D. Srinivas and E. B. Davies, Opt. Acta **28**, 981 (1981); L. Mandel, *ibid.* **28**, 1447 (1981).

[30]C. K. Hong, Z. Y. Ou, and L. Mandel, Phys. Rev. Lett. **59**, 2044 (1987); Z. Y. Ou and L. Mandel, *ibid.* **61**, 54 (1988); G. Rarity and P. R. Tapster, J. Opt. Soc. Am. B **6**, 1221 (1989).

[31]H. P. Yuen and J. H. Shapiro, in *Proceedings of the Fourth Rochester Conference on Coherence and Quantum Optics*, edited by L. Mandel and E. Wolf (Plenum, New York, 1978).

[32]See, e.g., F. A. M. de Oliveria, M. S. Kim, P. L. Knight, and V. Bužek, Phys. Rev. A **41**, 2645 (1990), and references therein.

[33]R. J. Glauber, Phys. Rev. **131**, 2766 (1963).

[34]J. D. Love and A. J. Ankiewicz, J. Light Wave Tech. **LT-3**, 100 (1985); A. W. Snyder and J. Fühl, *ibid.* **LT-3**, 31 (1985).